People Democratic Republic of Algeria

Ministry of Higher Education and Scientific Research

Ammar Telidji University-Laghouat

Faculty of Technology

Department of Electrical Engineering

Master's Thesis

Option: Electrical Control

Presented by

Imane AÏOUANA

Design of Fractional Order Adaptive Sliding Mode Observer for Induction Motor Drive

BIRAME. Mohammed	M.C.A	President
KOUZI Katia	Professor	Supervisor
BOUMEGOUAS Mohammed K.B	Doctoral student	Co-supervisor
AMER Aissa	Professor	Examiner
ABDERREZEK Hadjer	M.C.B	Examiner

2024/2025

الشُّكْر والتَّقدير

قال الله تعالى:
"يَرْفَعِ ٱللَّهُ ٱلَّذِينَ ءَامَنُواْ مِنكُمْ وَٱلَّذِينَ أُوتُواْ ٱلْعِلْمَ دَرَجَٰتٍۚ وَٱللَّهُ بِمَا تَعْمَلُونَ خَبِيرٌ"
(سورة المجادلة، الآية 11)

وقال رسول الله ﷺ:
"من سلك طريقًا يلتمس فيه علمًا، سهّل الله له به طريقًا إلى الجنة"
(رواه مسلم)

بقلوب ملؤها الامتنان والتقدير، أتوجه بخالص الشكر وعظيم العرفان لكل من ساندني في إنجاز هذا العمل المتواضع.

وأخصُّ بخالص الشكر وعظيم الامتنان مشرفتي الفاضلة الدكتورة كوزي كاتيا، على ما أولته لي من دعمٍ متواصل وجهدٍ صادقٍ وإرشادٍ علميٍّ نَيِّر، كان لها أبلغ الأثر في إثراء هذا البحث وإنجاحه، سائلةً المولى أن يجزيها عني خير الجزاء وأوفاه.

كما أشكر نائب المشرف، الأستاذ محمد الكبير بلال بومقواس، على متابعته وتوجيهاته سائلةً الله أن يجازيه ويبارك في علمه ووقته.

كما أتقدّم بالشكر لأساتذتي الكرام في كلية العلوم والتكنولوجيا جامعة عمار ثليجي، الذين لم يبخلوا بعلمهم ودعمهم، فكان لهم الفضل بعد الله فيما وصلت إليه.

ولا يسعني إلا أن أنحني تقديرًا واحترامًا لوالديّ الكريمين، على دعمهما غير المشروط، وصبرهما، ودعائهما المستمر، الذي كان نوري في كل مراحل حياتي.

كما أشكر إخوتي الذين كانوا لي سندًا وعونًا، وأحاطوني بالمحبة والتشجيع، فجزاهم الله عني خير الجزاء.

وختامًا، أحمد الله الذي وفقني وسدّد خطاي، وأسأله القبول والإخلاص.

"وَمَا تَوْفِيقِيٓ إِلَّا بِٱللَّهِۚ عَلَيْهِ تَوَكَّلْتُ وَإِلَيْهِ أُنِيبُ"
(سورة هود، الآية 88)

إهداء

قال الله تعالى:

"وَقُلْ رَبِّ ارْحَمْهُمَا كَمَا رَبَّيَانِي صَغِيرًا"

(سورة الإسراء، الآية 24)

بقلوبٍ يملؤها الوفاء، وأرواحٍ تفيض بالدعاء، أُهدي هذا الجهد المتواضع إلى من كانا لي سراجًا ينير طريق حياتي،

وأغدقا عليّ من واسع حنانهما وعظيم فضلهما، إلى والديّ العزيزين، أسأل الله أن يديم عليهما لباس الصحة والعافية، ويجزيهما

عني خير الجزاء وأوفاه .

وإلى إخوتي الأحبّاء، مروان وعبير ورشا، من تقاسمت معهم أطيب لحظات العمر، وكانوا لي سندًا لا ينضب من المحبّة والتشجيع، سائلة المولى أن يحفظهم بعين رعايته.

وإلى عائلتي الكريمة عيوانة، عائلة عماري، التي أفتخر بالانتماء إليها وأدين لها بما غرسته في داخلي من قيمٍ نبيلة ومبادئ راسخة، فلهم منّي أسمى مشاعر التقدير والعرفان.

وإلى روح جدّي العزيز وجدّتي الحبيبة، اللذين أضاءا حياتي بطيب دعائهما وحكمتهما، أسأل الله أن يتغمدهما بواسع رحمته ويدخلهما فسيح جنّاته.

وإلى جدّي وجدّتي حفظهما الله، سائلًا المولى أن يبارك في عمرهما ويُمتّعهما بموفور الصحة والعافية.

وإلى خالتي الغالية، من وجدت فيها قلبًا مملوءًا بالحنوّ والعطف، وكان لدعواتها ومساندتها الأثر الطيب في نفسي، فجزاها الله عني خير الجزاء وأوفاه.

وإلى صديقتي الوفية رتيبة، رفيقة الدرب وصاحبة المواقف النبيلة، التي أضاءت أيامي بصدق محبتها وإخلاصها، فأسأل الله أن يديم عليها سعادتها وتوفيقها .

وختامًا، أحمد الله تعالى على نعمه وتوفيقه، وأرجو منه القبول والإخلاص، فهو

نعم المولى ونعم النصير

عيوانة إيمان

الملخص

الهدف الرئيسي من هذا العمل هو تحسين أداء التحكم المتجه في السرعة بدون حساس للمحرك الحثي . في الجزء الأول، تم نمذجة المحرك الحثي إلى جانب مصدر تغذيته، والذي يتكون أساسًا من عاكس للجهد يتم التحكم فيه من خلال تنظيم التيار باستخدام تعديل عرض النبضة بالتباطؤ . بعد ذلك، تم عرض مبادئ التحكم المتجه كما تُطبق على المحرك الحثي.في المرحلة الثانية، تم اقتراح استراتيجية تحكم تآزري لتنظيم سرعة المحرك الحثي. وقد تم إجراء العديد من المحاكاة العددية لتوضيح وتحليل فعالية طريقة التحكم المقترحة.أما في المرحلة الأخيرة، ولتقليل ظاهرة الخفقان ، فقد تم تطوير نهج التحكم المتجه في السرعة بدون حساس باستخدام مراقب انزلاقي تكيفي من الرتبة الكسرية . يقوم المراقب المقترح باستبدال الحد المتقطع في المراقب التكيفي التقليدي بمصطلح تكاملي من الرتبة الكسرية ، مع الحفاظ على مزاياه. يقوم المراقب بتقدير مركبات الفيض الدوار في الإطار المرجعي الثابت اعتمادًا على الكميات القابلة للقياس في المحرك، بينما يتم تقدير السرعة الميكانيكية باستخدام دالة لياپانوف.

الكلمات المفتاحية: محرك حثي ، التحكم المتجه، منظمPI ، التحكم التآزري، مراقب انزلاقي تكيفي من الرتبة الكسرية، التكامل، دالة لياپانوف، المتانة.

Abstract

The main objective of this work is to enhance the performance of synergetic sensorless speed vector control for Induction Motor (IM). In the first part, the induction motor is modeled along with its power supply, which primarily consists of a voltage inverter controlled via current regulation using hysteresis PWM. Subsequently, the principles of vector control as applied to IM are presented. In the second phase, a synergetic control strategy is proposed for speed regulation of IM. Various numerical simulations are conducted to illustrate and analyze the effectiveness of the proposed control method. In the final phase, to reduce the chattering phenomenon, a sensorless speed vector control approach is developed using a fractional-order sliding mode adaptive observer. The proposed observer replaces the switching term in the conventional adaptive sliding mode observer with a fractional-order integral term, while preserving its advantages. The observer estimates the rotor flux components in the stationary reference frame based on the IM's measurable quantities, and the mechanical speed is estimated using a Lyapunov-based function.

Keywords- Induction Motor (IM); Vector Control; PI regulator; , Synergetic Control , Fractional order Adaptive Sliding Mode Observer, Integral, Lyapunov function, Robustness.

Résume

L'objectif principal de ce mémoire est d'améliorer les performances d'un contrôle découplé synergétique sans capteur de vitesse d'un moteur à induction triphasé (MI). Dans la première partie de ce travail, on a modélisé le moteur à induction et son alimentation constituée principalement par un onduleur de tension commandé en courant par MLI à hystérésis, puis on a présenté la technique de la commande à flux orienté et son application au MI. Dans une deuxième phase, on a exposé la stratégie de commande appliquée au MI. Plusieurs résultats de simulation numérique du contrôle présenté ont été illustrés et commentés. Dans la dernière phase, afin de minimiser le phénomène de broutement 'chattering' on a développé un contrôle vectoriel sans capteur de vitesse du MI associé d'un observateur d'ordre fractionnel adaptatif à mode glissement. L'idée de l'observateur proposé est de remplacer le terme discontinu de l'observateur adaptatif à mode glissement classique par un intégral d'ordre fractionnel tout en retient les avantages de ce dernier. L'observateur estime les flux rotoriques dans le référentiel lié au stator à partir les mesures du moteur. La vitesse de rotation mécanique est estimée par l'ajout d'une fonction de Lyapunov. Les performances et l'efficacité de l'algorithme de l'estimation proposée ont été illustrées par des résultats de simulation.

Mots clés : Moteur à Induction triphasé, Commande vectorielle, Régulateur PI classique, Contrôle synergétique, Observateur à Modes glissants Adaptatif d'ordre fractionnel, Intégral, Fonction de Lypunov, Robustesse.

Contents

List of Figures

List of Abbreviations

FOC	Field-Oriented Control
IM	Induction Motor
PI	Proportional–Integral
ASMO	Adaptive Sliding Mode Observer
FOASMO	Fractional Order Adaptive Sliding Mode Observer
VSI	Voltage Source Inverter

Notations

T_e	Electromagnetic torque [N · m]
T_L	Load (resistance) torque [N · m]
f	Network frequency [Hz]
i_{dqs}	Stator direct and quadrature current components [A]
i_{dqr}	Rotor direct and quadrature current components [A]
$i_{\alpha\beta s}$	Stator current components in stator reference frame [A]
J	Moment of inertia [kg · m²]
k	Discrete time step (index) [—]
k_1, k_2	Sliding mode observer gains [—]
K_p, K_i	Classical PI controller gains [—]
L_r	Rotor cyclic inductance [H]
L_s	Stator cyclic inductance [H]
f_r	Friction coefficient [N · s]
C	Filter capacitance [F]
L	Filter inductance [H]
M	Mutual inductance [H]
Ω	Mechanical rotor speed [tr/min]
ω_g	Slip angular frequency [rad/s or tr/min]
ω_s	Stator electrical angular frequency [rad/s or tr/min]
ω_r	Rotor electrical angular speed [rad/s or tr/min]
p	Number of pole pairs [—]
Ψ_{dqs}	Stator direct and quadrature flux components [Wb]
$\Psi_{\alpha\beta s}$	Rotor flux components in stator frame [Wb]
R_r	Rotor resistance [Ω]
R_s	Stator resistance [Ω]
σ	Blondel leakage coefficient [—]
σ_r	Inverse of rotor time constant [s^{-1}]
T_{ech}	Sampling period [s]

T_r	Rotor time constant [s]
θ	Rotor mechanical rotation angle [rad]
θ_s	Electrical angle of the rotating reference frame [rad]
$\hat{x}$	Estimated state [—]
ref	Reference value indicator [—]
v_{dqs}	Stator voltage direct and quadrature components [V]
v_{dqr}	Rotor voltage direct and quadrature components [V]
$v_{\alpha\beta s}$	Stator voltage components in stator frame [V]
`sign(s)`	Sign function
μ	Relative degree (order of sliding mode control)
h	Time increment
x_f	Time-dependent function
$f(x, u, t)$	A nonlinear function
x, u	State vector and Control vector
$\psi(x, t)$	A function described by the user
ψ	Macro-variable
T	Synergetic observer time constant
K_i	Synergetic observer gains
$u(t)$	Control input
$y(t)$	System output
X_i	Positions for Bat Algorithm
e	Difference between reference value and actual value

GENERAL INTRODUCTION

PROBLEM FORMULATION

Due to its robustness, the simplicity of its structure, its low cost, and which does not need a regular maintenance, the induction motor (IM) offers technological prospects in many industrial fields [1]. However, the IM presents a nonlinear model and strongly coupled formally due to the absence of the natural decoupling between the different input-output variables which complicates its control. The control complexity of this machine has paved the way for several control strategies, which the most popular is the vector control in its different versions. Vector control offers good performance during transient and permanent phases. The first controllers used are the PIDs. They have the advantage of simplicity of implementation and ease of synthesis. Nevertheless, they have poor robustness with respect to the machine parameter variations [2].

Synergetic control has emerged only in recent years and shares a conceptual approach with sliding mode control, making it a powerful methodology for robust control design. This synergistic technique not only reduces the complexity of the system model but also generally ensures the stability of the controlled system. Synergetic control theory offers several advantages: it is well-suited for digital control applications, operates at a constant switching frequency, simplifies filter design, and reduces chattering phenomena, all while preserving the inherent robust characteristics of sliding mode control [2]. Moreover, field oriented control of IM relies heavily on knowledge of mechanical speed and flux. As a result, there has been increasing industrial interest in high-performance IMs that operate without sensors in recent years. These sensorless systems offer numerous benefits, including lower costs, reduced maintenance, and enhanced reliability. Sliding mode observers are considered an attractive choice due to their robustness against parameter variations, external disturbances, and fast convergence [3]. However, conventional sliding mode observers, based on variable structure control theory, suffer from a notable drawback: the estimated values often exhibit high-frequency chattering. This chattering arises from the use of finite feedback gain and the discontinuous nature of the control input, which can induce torque oscillations and excite unmodeled high-frequency dynamics or mechanical resonances. To address this issue, various solutions

have been proposed to strike a balance between minimizing chattering and maintaining observer robustness. Regarding of above point, we propose in this work simple but powerful Fractional Order Adaptive Sliding Mode Observer for IM (FOSMO) witch able to reduce the high-frequency chattering, and retain the benefits achieved in the conventional sliding observer. The suggested observer uses the stator current error and its integral to replace the discontinuity observer term. Fractional calculus methods have become increasingly popular in engineering applications due to their ability to enable more effective control of systems. The choice of fractional order must be based on the specific problem's structure. Consequently, various definitions of fractional calculus have been developed, with the Riemann-Liouville and Caputo definitions being the most commonly used in engineering applications. For IM applications, fractional integral order calculus offers notable advantages, such as increased robustness and non-sensitivity to parameter variations [4]. Based on above point, in this work we propose a robust synergetic decoupled control of IM based on fractional order adaptive sliding-mode observer.

OUTLINE OF THE THESIS

The present work is constructed by three chapters given as follows: The first chapter is dedicated to the modeling of the induction motor (IM) in the d–q reference frame, along with its power supply, which consists of a voltage inverter controlled by pulse-width modulation (PWM). Additionally, the application of indirect vector control to the IM is thoroughly explained. The chapter concludes with simulation results that demonstrate the performance of the vector control strategy. The second chapter presents the design of a robust synergetic controller for IM speed regulation. Various digital simulations are provided to validate the effectiveness and robustness of the proposed control strategy. The last chapter focuses on the design of a fractional-order adaptive sliding mode observer for speed IM estimation. The proposed observer estimates the rotor flux components in the stationary reference frame, while the motor speed is estimated using a Lyapunov-based approach. The effectiveness of the estimation algorithm is evaluated under various operating conditions using a dedicated sensorless IM benchmark and the MATLAB/Simulink simulation environment. To conclude this work, a general summary is presented, and several perspectives for future research and development are proposed.

Bibliography

[1] A.Zorig,A. Belkheiri, M. Belkheiri, K.Kouzi . *ADRC control of an induction motor with varying parameters*, 19th International Multi-Conference on Systems, Signals Devices (SSD),2022, DOI: 10.1109/SSD54932.2022.9955792.

[2] M. K. B.Boumegouas K. KouziM. Birame. *Robust synergetic control of electric vehicle equipped with an improved load torque observer.*In International Journal International Journal of Emerging Electric Power Systems, 2023.

[3] Tursini, M., Petrella, R., and Parasiliti, F. *Adaptive Sliding-Mode Observer for Speed-Sensorless Control of Induction Motors.*IEEE Tran. Ind. Applicat., Vol. 36, No.5, Sep./Oct 2000, pp. 1380-1387.

[4] E. Ilten. *Fractional order weighted mixed sensitivity-based robust controller design and application for a nonlinear system.*Fractal, vol. 7, no. 10, p. 769, Oct. 2023.

Chapter 1

Induction motor modeling and vector control

1.1 Introduction

The asynchronous motor, also known as the induction motor, is one of the most widely used electrical machines in industrial applications. It operates on alternating current (AC) and is characterized by the absence of direct contact between the stator and rotor. The term "asynchronous" refers to the fact that its rotational speed does not necessarily match the synchronous speed determined by the supply frequency. Historically, asynchronous machines faced competition from synchronous machines in high-power applications. However, advancements in power electronics have significantly enhanced their performance, making them the preferred choice in various industries.

Induction motors are particularly valued for their robustness, cost-effectiveness, and minimal maintenance requirements, making them highly suitable for applications requiring speed control and energy efficiency. [6]

1.2 Induction motor model

The mathematical model of an electric machine represents the real machine, allowing for the simulation of behaviors observed in experiments. This model plays a crucial role in solving technical issues associated with induction motors and greatly facilitates their analysis and design.

1.2.1 IM Modeling in the Three-phase abc frame

Consider a three-phase induction machine with its stator and rotor schematically represented in the following figure :

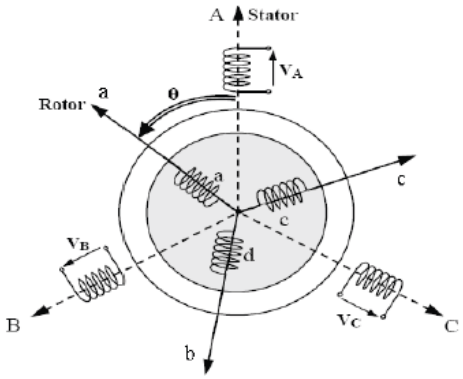

Figure 1.1: Schematic representation of a three-phase induction motor

The voltage equations

For the stator

$$[U_{s,ABC}] = R_s[I_{s,ABC}] + \left[L_s \frac{d}{dt}[I_{s,ABC}]\right] + \frac{d}{dt}\left([L_m][I_{r,ABC}]\right) \tag{1.1}$$

For the rotor

$$[U_{r,ABC}] = R_r[I_{r,ABC}] + \left[L_r \frac{d}{dt}[I_{r,ABC}]\right] + \frac{d}{dt}\left([L_m][I_{s,ABC}]\right) \tag{1.2}$$

These equations reveal a relationship between the variables, indicating non-linearity, which complicates the control of the induction motor. To overcome this challenge, we will use the Park transformation.

1.3 Application of the Park transformation on three-phase induction motor

Park transformation involves changing the reference axes to align with the two windings of the original machine, followed by a rotation that creates electrically and magnetically equivalent windings. This approach ensures that the mutual inductances of the model are no longer dependent on the rotation angle [5]. This transformation, which facilitates the conversion from a three-phase system to a two-phase (d, q) system, is known as the Park transformation and is represented as follows :

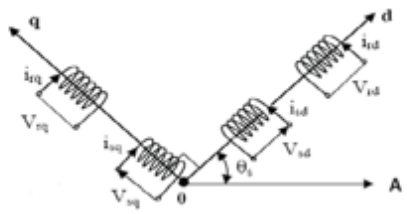

Figure 1.2: Schematic representation equivalent d-q Axis Model of an Induction Motor

Equation :

$$[U_{dq0}] = [A][U_{abc}] \tag{1.3}$$

$$[i_{dq0}] = [A][i_{abc}] \tag{1.4}$$

$$[\varphi_{dq0}] = [A][\varphi_{abc}] \tag{1.5}$$

With

$[A]$ is the Park matrix.

$$[A] = \frac{2}{3}\begin{bmatrix} \cos\theta & \cos\left(\theta - \frac{2\pi}{3}\right) & \cos\left(\theta + \frac{2\pi}{3}\right) \\ -\sin\theta & -\sin\left(\theta - \frac{2\pi}{3}\right) & -\sin\left(\theta + \frac{2\pi}{3}\right) \\ \frac{1}{2} & \frac{1}{2} & \frac{1}{2} \end{bmatrix} \tag{1.6}$$

1.3.1 State form of the induction motor model in the mark (d, q) Linked to the rotating field

Assuming linear magnetic circuits and a sinusoidal distribution of air-gap flux density, the induction motor's equivalent two-phase model, represented in the synchronous (d, q) reference frame and formulated in state-space form, is a fourth-order model [13] :

$$\dot{x} = Ax + Bv_s \tag{1.7}$$

Where

$$x = \begin{bmatrix} \Psi_d & \Psi_q & i_s \end{bmatrix}^T, \quad i_s = \begin{bmatrix} i_d & i_q \end{bmatrix}^T, \quad \phi_s = \begin{bmatrix} \phi_d & \phi_q \end{bmatrix}^T, \quad v_s = \begin{bmatrix} V_d & V_q \end{bmatrix}^T \tag{1.8}$$

The system matrices are given by:

$$A = \begin{bmatrix} -\frac{1}{\sigma L_s}\left(R_s + \frac{M^2}{L_r}\sigma_r\right) & \omega_s & \frac{M}{\sigma L_s L_r} & \frac{PM}{\sigma L_s L_r} & \sigma_r \\ -\omega_s & -\frac{1}{\sigma L_s}\left(R_s + \frac{M^2}{L_r}\sigma_r\right) & \frac{PM}{\sigma L_s L_r} & \frac{M}{\sigma L_s L_r} & -\sigma_r \\ M\sigma_r & 0 & 0 & \omega_s - P\omega_r & \sigma_r \\ M\sigma_r & 0 & -(\omega_s - P\omega_r) & 0 & -\sigma_r \end{bmatrix}$$

$$B = \begin{bmatrix} \frac{1}{\sigma L_s} & 0 \\ 0 & \frac{1}{\sigma L_s} \\ 0 & 0 \\ 0 & 0 \end{bmatrix}$$

Where

$$\sigma = 1 - \frac{M^2}{L_s L_r}, \quad \sigma_r = \frac{R_r}{L_r} \tag{1.9}$$

The mechanical modeling part of the system is given by:

$$J\frac{d\omega_r}{dt} = T_{em} - T_l - K_f\omega_r \quad (1.7) \tag{1.10}$$

$$T_{em} = \frac{3}{2}P\frac{M}{L_r}(\phi_d i_q - \phi_q i_d) \quad (1.8) \tag{1.11}$$

1.3.2 Model of induction motor in mark linked to the stator

$$\frac{d}{dt}\begin{bmatrix} \bar{i}_s \\ \bar{\phi} \end{bmatrix} = \begin{bmatrix} A_{11} & A_{12} \\ A_{21} & A_{22} \end{bmatrix}\begin{bmatrix} \bar{i}_s \\ \bar{\phi} \end{bmatrix} + \begin{bmatrix} b \\ 0 \end{bmatrix}\bar{v}_s$$

$$\frac{dx}{dt} = Ax + Bv_s \quad \text{state equation.}$$

$$y = \bar{i}_s = Cx \quad \text{Output equation.}$$

$$\bar{x} = \begin{bmatrix} \bar{i}_s \\ \bar{\phi} \end{bmatrix} \quad \text{state vector.}$$

With:

$$\bar{i}_s = \begin{bmatrix} i_{s\alpha} \\ i_{s\beta} \end{bmatrix} \quad \text{stator current vector.}$$

$$\bar{\phi}_r = \begin{bmatrix} \phi_{r\alpha} \\ \phi_{r\beta} \end{bmatrix} \quad \text{Rotor current vector.}$$

$$\bar{v}_s = v_s = \begin{bmatrix} v_{s\alpha} \\ v_{s\beta} \end{bmatrix} \quad \text{state voltage vector.}$$

$$a_{r\,11} = -\left(\frac{R_s}{\sigma L_s} + \frac{M^2 \sigma_r}{\sigma L_s L_r}\right) \tag{1.12}$$

$$A_{11} = a_{r\,11} I \tag{1.13}$$

$$A_{12} = \frac{M}{\sigma L_s L_r}(\sigma_r I - \omega_r J) = a_{r\,12} I - a_{i\,12} J \tag{1.14}$$

$$A_{21} = a_{r\,21} I, \quad a_{r\,21} = \sigma_r M, \tag{1.15}$$

$$A_{22} - \sigma I + \omega_r J = a_{r\,22} I + a_{i\,12} J, \tag{1.16}$$

$$I = \begin{bmatrix} 1 & 0 \\ 0 & 1 \end{bmatrix}, \quad J = \begin{bmatrix} 0 & -1 \\ 1 & 0 \end{bmatrix}$$

$$b = b_1 I, \quad b_1 = \frac{1}{\sigma L_s}$$

$$\begin{bmatrix} I & 0 \end{bmatrix} \quad \text{Output Matrix;}$$

Q and I: Identity and dim zero matrices 2×2.

1.3.2 Modeling of the induction motor - voltage inverter association

Generally, two cascaded converters power the asynchronous machine. On the machine side, an MLI voltage inverter is used, while on the network side, a three-phase diode rectifier is employed, separated by an LC low-pass filter, as shown below:

Each switch C is associated with a logical function F_i $(i = 1, 3)$, such that:

- If $F_i = 1$, then phase a is connected to the positive terminal of the DC source E.
- If $F_i = -1$, then phase a is connected to the negative terminal of the DC source E.

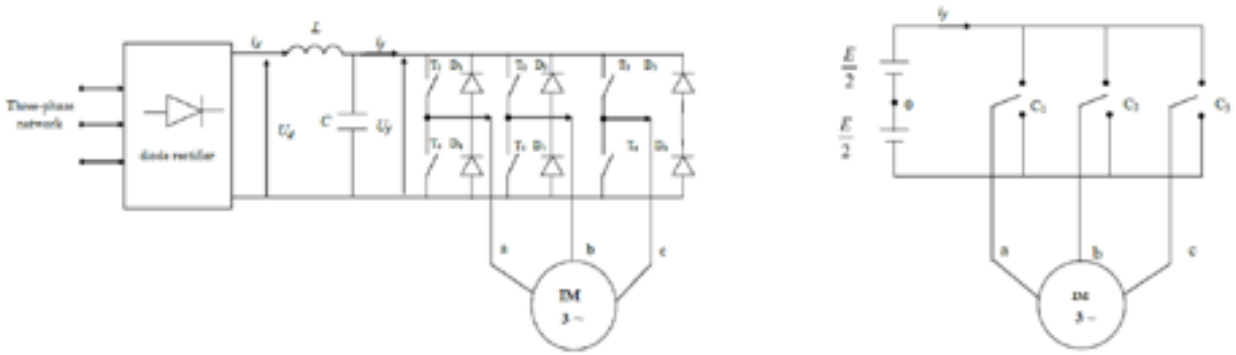

Figure 1.3: Diagram of the induction motor - voltage inverter by switches association

It follows that

$$U_{ab} = \frac{1}{2}(F_1 - F_2)E \tag{1.17}$$

$$U_{bc} = \frac{1}{2}(F_2 - F_3)E \tag{1.18}$$

$$U_{ca} = \frac{1}{2}(F_2 - F_1)E \tag{1.19}$$

The simple stator voltages are obtained from equation (1.11) as follows:

$$\begin{bmatrix} U_{ca} \\ U_{cb} \\ U_{cc} \end{bmatrix} = \frac{E}{3} \begin{bmatrix} 2 & -1 & -1 \\ -1 & 2 & -1 \\ -1 & -1 & 2 \end{bmatrix} \begin{bmatrix} F_1 \\ F_2 \\ F_3 \end{bmatrix}$$

The current at the input of the inverter has the expression:

$$i_f = F_1 i_a + F_2 i_b + F_3 i_c$$

The determination of the logical functions F_i $(i = 1, 3)$ depends on the control strategy. In our case, we use the hysteresis pulse width modulation (MLI) control technique [7].

1.3.3 Hysteresis PWM Control

The hysteresis MLI control ensures that the phase current closely follows the reference current. By enforcing sinusoidal currents in the asynchronous machine, a constant electromagnetic torque is maintained. The simplest method to achieve this involves comparing the measured phase current with the reference current using a hysteresis comparator. This comparator generates pulses that trigger and block the inverter switches, keeping the phase current within a hysteresis band of $\pm 2\Delta i$ around the reference current [11].

The switching states of the three static switches $F_i(i = 1, 3)$ of the inverter are determined by the corresponding logical states as follows:

$$F_i = -1 \quad \text{if} \quad i_i \geq i_{\text{ref}} + \Delta i \tag{1.20}$$

$$F_i = 1 \quad \text{if} \quad i_i \leq i_{\text{ref}} - \Delta i \tag{1.21}$$

$$F_i = F_{(i-1)}, \quad i_i = i_{\text{ref}} \tag{1.22}$$

Where:

- $i(i = 1, 3)$: represents the currents of the stator phases (i_a, i_b, i_c).
- $i_{\text{ref}}(i = 1, 3)$: are the reference currents corresponding to the three arms of the inverter.
- Δi: denotes the hysteresis band, which is chosen to keep the switching frequency of the controlled semiconductors within acceptable limits while effectively minimizing current harmonics [8].

1.3.4 SIMULATION RESULTS AND DISCUSSION

The numerical solution of the differential equations (state space) and the dynamic equation was achieved using MATLAB software. The parameters of the induction motor used in the simulation are provided in Appendix (A). Two tests were conducted:

1.3.5 Operating without load

Figure (1.3) illustrates the evolution of the IM characteristics during no-load operation ($T_r = 0$):

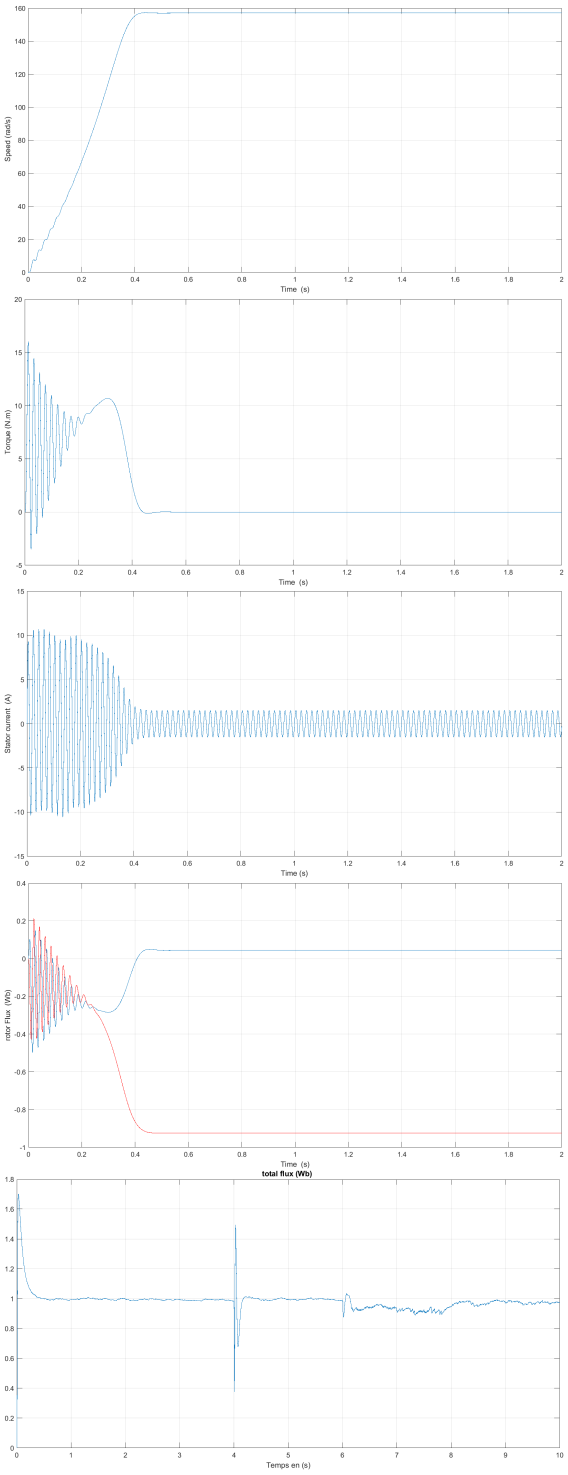

Figure 1.4: Dynamic and static Characteristic of IM without load torque

1.3.6 Operating with load $T_r = 5\,\mathbf{N \cdot m}$

Figure (1.3) illustrates the evolution of the IM characteristics during loaded operation with $T_r = 5\,\mathrm{N \cdot m}$ applied at $t = [0.8, 1.2]$ s.

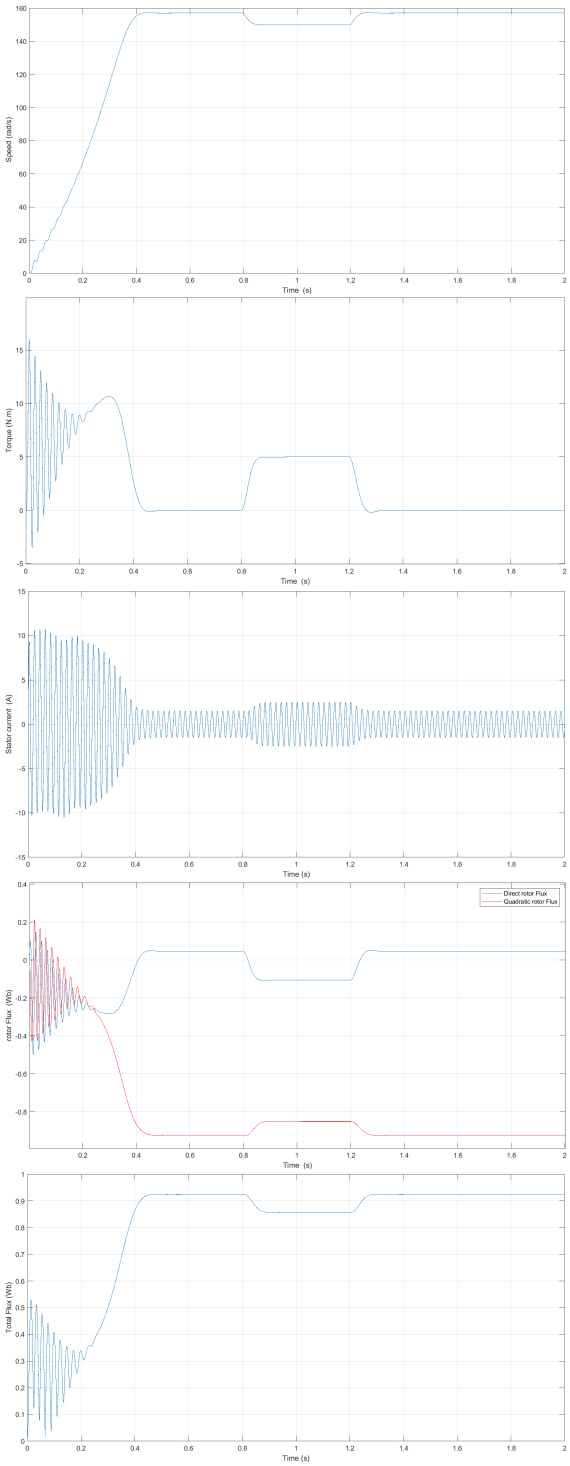

Figure 1.5: IM characteristics during load application $T_r = 5N.m$ at $t = [0.8 - 1.2]s$

Discussion

These results demonstrate the effectiveness of the Field-Oriented Control (FOC) strategy in maintaining the motor's performance under varying load conditions. The control system successfully regulates the current and torque, ensuring smooth operation and quick stabilization after disturbances.

1.4 IM Control technique

1.4.1 Introduction

In recent decades, induction motor control has been a major area of research and development. One of the key innovations in this domain is Vector Control (VC), which utilizes partial feedback linearization along with a proportional-integral (PI) controller to regulate the motor's state. The following section will explore the core principles of vector control and its application to induction motors [9].

1.4.2 Principle of flux orientation control (F.O.C)

An analysis of the asynchronous machine's torque expression reveals that it is derived from the product difference between two quadrature components: the rotor flux and the stator currents. This relationship creates complex coupling between the machine's variables. The primary goal of flux orientation control is to decouple the components responsible for magnetization and torque production.Mathematically, the control strategy involves performing transformations to convert the inherently nonlinear system into a linear one, thus ensuring independence between flux generation and torque production, similar to a separately excited direct current machine. Flux orientation control achieves this by regulating the flux using one current component and controlling the torque with another.To implement this approach, it is necessary to select an appropriate "d, q" axis system. By strategically choosing the orientation angle of the "d, q" reference frame, the "d" axis can be aligned with the resultant flux, effectively eliminating the transverse flux component. This alignment can be achieved by choosing the reference axes based on one of the machine's fluxes, such as the stator flux, rotor flux, or air gap flux. This choice determines the conditions for flux orientation as follows:

Stator flux

$$\phi_{sd} = \phi_s \text{ and } \phi_{sq} = 0 \tag{1.23}$$

Air gap flux

$$\phi_{rd} = \phi_r \text{ and } \phi_{mq} = 0 \tag{1.24}$$

Rotor flux

$$\phi_{rd} = \phi_r \text{ and } \phi_{rq} = 0 \tag{1.25}$$

In the three reference systems, the torque is proportional to the flux product by the current component i_{qs}, but only the choice of rotor flux allows a decoupling characterized by an independence of flux and current component in quadrature with flux. Moreover, this choice makes it possible to have a high starting torque, which justifies the use of this type of flux orientation [13].

Vector control types

There are two main types of vector control:

- The direct vector control
- The indirect vector control

The direct Vector control This control method was introduced by Blaschke. It requires knowledge of the flux magnitude and its phase to achieve decoupling between torque and flux, regardless of the operating point. Sensors can be used to obtain information about the flux's amplitude and phase. However, a drawback of this approach is that these sensors are mechanically fragile and cannot function effectively under harsh conditions, such as vibrations or extreme heat.

The indirect Vector control The principle of this method is to avoid measuring (or estimating) the flux amplitude and instead focus solely on determining its position. This concept, proposed by Hasse, involves estimating the position of the flux vector. The method gained popularity with the advancement of microprocessors; however, it is highly sensitive to the machine's parameter variations. It is worth noting that the indirect method is simpler and more widely used than the direct method, although the choice between the two depends on the specific application [11].

Induction Motor Current Model

By assuming the frequency converter to be ideal and neglecting the effect of stator dynamics, the current-fed asynchronous machine model can be derived. This model is represented by the following two rotor voltage equations:

$$R_r i_{rd} + \frac{d\phi_{rd}}{dt} - (\omega_s - \omega_r)\phi_{rq} = 0 \tag{1.20}$$

$$R_r i_{rq} + \frac{d\phi_{rq}}{dt} - (\omega_s - \omega_r)\phi_{rd} = 0 \tag{1.26}$$

The rotor flux model is expressed in state-space form, where the stator currents are imposed, as follows:

$$\frac{d\phi_{rd}}{dt} = -\frac{1}{T_r}\phi_{rd} + \omega_{gl}\phi_{rq} + \frac{M}{T_r}i_{sd} \tag{1.21}$$

$$\frac{d\phi_{rq}}{dt} = -\frac{1}{T_r}\phi_{rq} + \omega_{gl}\phi_{rd} + \frac{M}{T_r}i_{sq} \tag{1.27}$$

$$J\frac{d\Omega_r}{dt} = C_{em} - C_r - f_r\Omega_r \tag{1.28}$$

With: $\omega_{gl} = \omega_s - \omega_r$

Furthermore, to achieve vector control through rotor flux orientation, the following conditions must be met:

$$\phi_{rq} = 0 \quad \text{and} \quad \dot{\phi}_{rq} = 0$$

$$\phi_{rd} = \phi_r \quad \text{and} \quad \dot{\phi}_{rd} = \dot{\phi}_r$$

Thus, the system of equations (1.21) and equation (1.8) become:

$$\frac{d\phi_r}{dt} = -\frac{1}{T_r}\phi_r + \frac{M}{T_r}i_{sd} \tag{1.29}$$

$$C_{em} = \frac{3}{2}p\frac{M}{L_r}i_{sq}\phi_r \tag{1.22}$$

$$\omega_{gl} = \frac{M}{T_r}\frac{i_{sq}}{\phi_r} \tag{1.30}$$

It is observed that the torque equation is similar to that of a separately excited DC machine, allowing for independent control of torque and flux. [6] [10]

1.4.3 Speed regulation of the IM controlled vector by a conventional PI

The block diagram of the speed control for an induction motor drive using field-oriented control with a conventional PI regulator is shown in the following figure:

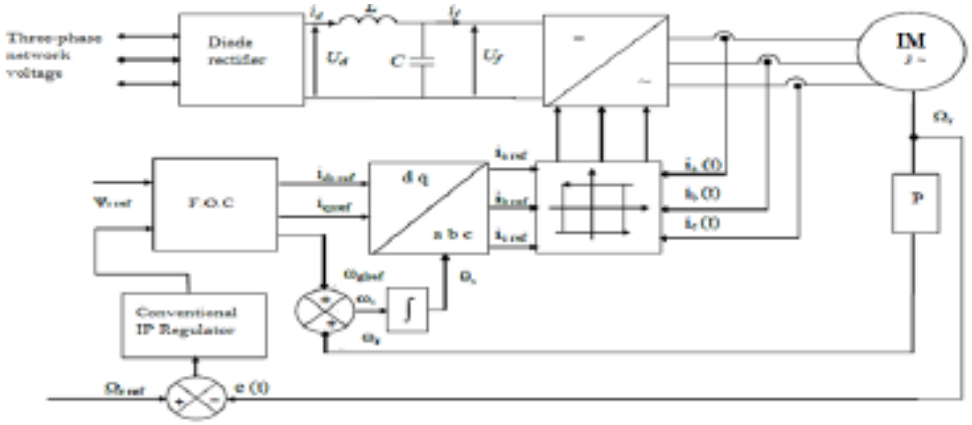

Figure 1.6: Indirect vector control of IM

1.4.4 Simulation results and discussion

To demonstrate the enhancement of the overall dynamics of the control system, various tests were conducted to evaluate the performance of the implemented control. The proportional-integral (PI) regulator was configured with the following parameters kp = 0.5 and ki=3.06 Initially, from t=0 to t=0.8 , no load was applied. Subsequently, from t=0.8 to t=1.2, a load of Cr =5N/m was introduced, resulting in a noticeable disturbance in the system The effect of Cr on the rotational speed was observed. To assess the robustness of the control system, a speed variation test was conducted from t=4 to =6 At t=8, the motor was restarted with a rotational speed of 10 tr/min.

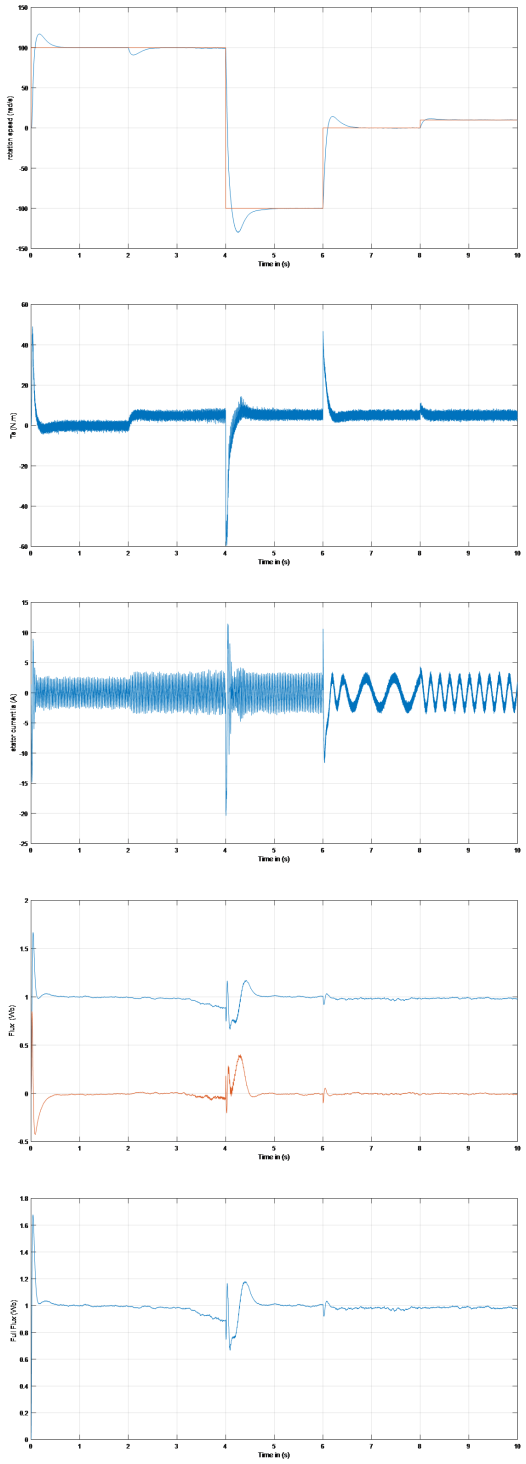

Figure 1.7: Performances IM vector control with classical PI of 1.2.

1.4.5 1.4.7 Robustness Test

Simulation Results and Discussion

This section presents the performance analysis of an induction motor controlled by Field-Oriented Control (FOC) using a PI regulator, including robustness tests to examine its effectiveness and limitations.

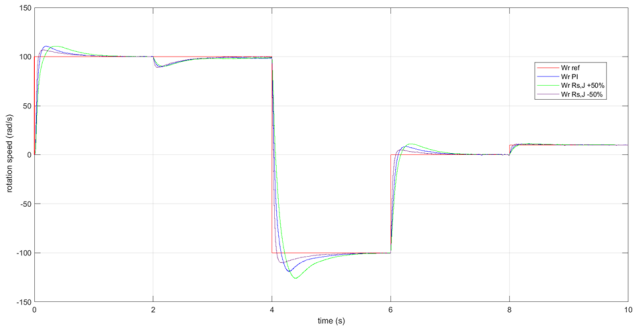

Figure 1.8: Robustness Test of Rotor Speed Using PI Controller

Discussion:

These figures illustrate the impact of load disturbances on the system. It is clear that the PI regulator does not handle such disturbances effectively and is sensitive to parametric variations. Therefore, we implement synergetic control to assess and improve the system's performance.

1.5 Conclusion

This chapter presented the modeling of the induction motor (IM) along with its power supply. The concept of vector control for the induction machine was then introduced. Simulation results demonstrated that while classical PI control provides satisfactory performance in vector control, its sensitivity to disturbances and parameter variations limits its robustness. To overcome these limitations, the next chapter will focus on the integration of Synergetic Control.

Bibliography

[5] Ould Sass Mohamed, *Commande synergétique d'un moteur asynchrone*. Master's thesis, University of Annaba, Annaba, Algeria.

[6] B. K. Bose, *Modern Power Electronics and AC Drives*. Upper Saddle River, NJ, USA: Prentice Hall, University of Tennessee - Knoxville (UTK), 2001.

[7] B. K. Bose, *Power Electronics and Motor Drives: Advances and Trends*. Amsterdam, Netherlands: Academic Press, 2006.

[8] D. G. Holmes and T. A. Lipo, *Pulse Width Modulation for Power Converters: Principles and Practice*. Piscataway, NJ, USA: IEEE Press, 2003.

[9] P. C. Krause, O. Wasynczuk, and S. D. Sudhoff, *Analysis of Electric Machinery and Drive Systems*, 3rd ed., Hoboken, NJ, USA: Wiley-IEEE Press, 2013.

[10] W. Leonhard, *Control of Electrical Drives*, 3rd ed. Springer, 2001.

[11] K. Kouzi, *Contribution des techniques de la logique floue pour la commande d'une machine à induction sans transducteur rotatif*. Master's thesis, University of Elhadj Lakhdar, Batna, Algeria.

[12] K. Kouzi, L. Mokrani, and M.-S. Naït-Saïd, "A new design of fuzzy logic controller with fuzzy adapted gains based on indirect vector control for induction motor drive," in *IEEE-SSST Annual Meeting*, West Virginia, USA, March 2003.

[13] K. Kouzi, L. Mokrani, and M.-S. Naït-Saïd, "High performances of fuzzy self-tuning scaling factor of PI fuzzy logic controller based on direct vector control for induction motor drive without flux measurements," in *Proceedings of the IEEE International Conference on Industrial Technology (ICIT)*, December 2004.

Chapter 2

Synergetic Vector Control Applied to Induction Motors

2.1 Introduction

In the previous chapter, the modeling of the induction motor (IM), along with the implementation of vector control to enhance its dynamic performance. While the classical PI controller has been widely used in vector control due to its simplicity and effectiveness, its sensitivity to parameter variations and external disturbances limits its robustness. To address these limitations, this chapter introduces Synergetic Control, a modern control strategy derived from the principles of synergetics and nonlinear control theory. Unlike traditional PI control, Synergetic Control ensures global system stability and improved dynamic response by designing control laws that guide the system's trajectory toward a predefined manifold. This approach enhances the motor's robustness and adaptability to variations in operating conditions. The chapter begins with an overview of the fundamental concepts of Synergetic Control, followed by its mathematical formulation and application to the IM model. The design of the control law, including the selection of appropriate system parameters, is detailed to ensure optimal performance. Finally, simulation results are presented to compare the effectiveness of Synergetic Control with conventional PI-based vector control, demonstrating its advantages in terms of robustness and disturbance rejection [18].

2.2 Synergetic Control Approach

The Sliding Mode Control (SMC) strategy has been widely used in numerous industrial applications due to its robustness. However, it is significantly hindered by a major drawback—chattering, a phenomenon caused by high frequency switching that leads to steady-

state errors and can damage actuators [15]. To address this issue, Professor A. Kolesnikov introduced an innovative method known as Synergetic Control (SC) Theory. This modern control approach is grounded in the principles of goal-oriented self-organization and leverages the dynamic characteristics of nonlinear systems. Synergetic control enables effective handling of complex control problems that have proven challenging or even unsolvable using traditional or previously proposed techniques [16].
In recent years, SC has gained considerable attention in the field of electrical machine control, emerging as a strong candidate to replace SMC due to its enhanced robustness and performance. Some of its key advantages include [17]:

- High robustness to parameter variations
- Superior performance compared to conventional PI regulators
- Invariance to load disturbances
- Minimal system vibrations
- Effective in digital (numerical) control implementations

2.2.1 Synergetic Controller Design Steps

Typically, the nonlinear dynamic system is modeled using the following equation [14]:

$$\dot{x} = f(x(t), u(t)) \tag{2.1}$$

Where:
x(t) represents the state variables.
u(t) is the control vector.

The design of a synergetic controller involves several key steps, outlined as follows:

1. The initial step involves selecting macro-variables based on the system variables. These macro-variables define the system's motion properties and should not exceed the number of controlled variables. Each macro-variable imposes a new constraint on the system within its state space, effectively reducing its order by one unit and guiding it toward the globally stable desired state.

$$\Psi = \Psi\left(x(t)\right) \tag{2.2}$$

Where:
Ψ is the macro-variable, and $\Psi(x(t))$ is a function defined by the control designer.

2. Second step: Directing the dynamic evolution of macro-variables to the manifolds ($\psi = 0$) according to the following formula:

$$T\dot{\Psi} + \Psi = 0 \quad \text{with} \quad T > 0 \tag{2.3}$$

3. Finally: Determine the control law by resolving the mathematical equations by substitution of equation (2.1) and equation (2.2) in equation (2.3), we obtain:

$$T\frac{d\psi}{dx}f(x,u,t) + \psi = 0 \tag{2.4}$$

So, the control law is obtained as follows:

$$u = g\left(x, \psi(x,t), T, t\right) \tag{2.5}$$

2.2.2 Synergetic Speed Controller Design

In the first chapter, a classical PI controller is commonly used in the outer speed loop to generate the reference torque. In this study, we propose a novel robust controller design based on synergetic control [15]. The speed controller is responsible for generating the reference torque T_{ref}, with the speed error defined as:

$$e(t) = \Omega_{\text{ref}} - \Omega_r = 0 \tag{2.6}$$

The first step of Synergetic Control (SC) is choosing the macro-variable of the induction motor (IM) speed as follows [19]:

$$\psi_\Omega = k_P(\Omega_{\text{ref}} - \Omega_r) + k_I \int (\Omega_{\text{ref}} - \Omega_r)\, dt \tag{2.7}$$

Where k_P and k_I are the proportional and integral parameters of the speed macro-variable. The derivative of the speed macro-variable is given by:

$$\dot{\psi}_\Omega = k_P\dot{\Omega}_{\text{ref}} + k_I(\Omega_{\text{ref}} - \Omega_r) \tag{2.8}$$

The control law must satisfy the following equation:

$$T\dot{\psi}_\Omega + \psi_\Omega = 0 \quad \text{with} \quad T > 0 \tag{2.9}$$

The dynamic equation is given as:

$$\dot{\Omega} = \frac{1}{J}(T_{em} - T_r - K_f\Omega) \tag{2.10}$$

By substituting Eq. (2.10) into Eq. (2.9), and based on the synergetic control theory, we can write:

$$T\left[k_P \cdot \frac{1}{J}(T_{em} - T_r - K_f\Omega) + k_I(\Omega_{\text{ref}} - \Omega_r)\right] + k_P(\Omega_{\text{ref}} - \Omega_r) + k_I \int (\Omega_{\text{ref}} - \Omega_r)\, dt = 0 \quad (2.11)$$

Solving for the control input (electromagnetic torque), we obtain:

$$T^*_{em} = \frac{J}{Tk_P}\left[\frac{Tk_P}{J}T_r + \frac{Tk_P}{J}K_f\Omega - Tk_I(\Omega_{\text{ref}} - \Omega_r) - k_P(\Omega_{\text{ref}} - \Omega_r) - k_I \int (\Omega_{\text{ref}} - \Omega_r)\, dt\right] \quad (2.12)$$

The synergetic control law must ensure the stability of the closed-loop speed control. One can use the following Lyapunov function:

$$V = \frac{1}{2}\psi(e)^2 \quad (2.13)$$

After differentiation, one gets:

$$\dot{V} = \psi(e) \cdot \dot{\psi}(e) \quad (2.14)$$

Using the synergetic condition from Eq. (2.9), we obtain:

$$\dot{V} = -\frac{1}{T}\psi(e)^2 \quad (2.15)$$

Thus, the inequality in Eq. (2.15) ensures the stability of the closed-loop speed control system.

2.2.3 Application of Synergetic Speed Control for IM

To derive the desired control law, the initial step in designing the synergetic controller involves selecting appropriate macro-variables. Typically, these macro-variables are defined as functions of the system's state variables. The goal is to formulate a control law based on state functions, such as speed Ω and flux φ, in order to generate the reference values needed for the motor's speed ψ_{ref} and flux ψ_{ref}.

Therefore, torque control must be ensured. To address this issue, the previously described method is applied—specifically, determining a control law $u(\Omega, \varphi)$. The first step involves selecting suitable macro-variables, which can generally be any function (including nonlinear ones) of the state variables. In this context, we consider three components: Ω_r, i_{ds}, and i_{qs}, which allow us to impose the following invariants: a technological constraint $\Omega_r = \text{const}$, and electromagnetic constraints $\varphi_{dr} = \text{const}$, $\psi = 0$ [19].

2.2.4 Simulation results of the synergetic control

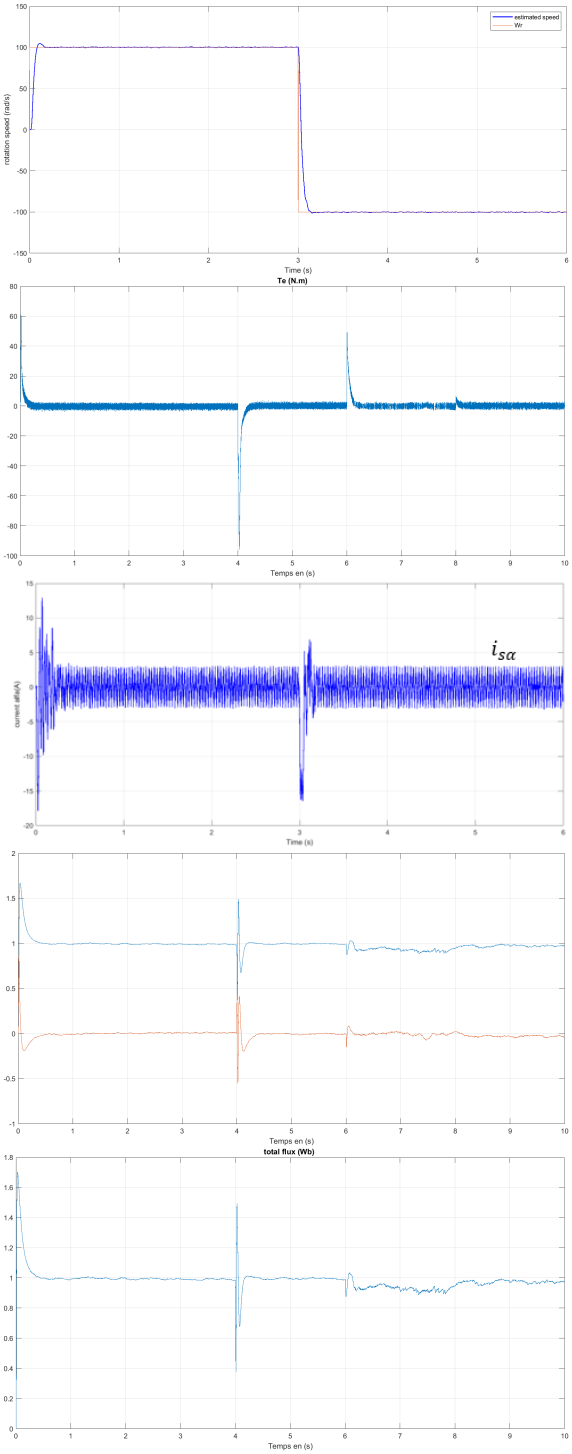

Figure 2.1: Performance Evaluation of Synergetic Control of IM

discussion

The application of synergetic control to the induction motor (IM) demonstrates both the simplicity of its design and its improved performance over conventional control methods. Its effectiveness is clearly shown through the elimination of the quadrature flux component and its ability to replicate the behavior of a separately excited DC motor. In addition, synergetic control consistently provides reliable and stable performance, even under sudden variations in speed reference and in the presence of load torque disturbances.

2.3 conclusion

This chapter focused on the design and application of a SC strategy for regulating the speed of an IM using vector control. A major strength of SC lies in its ability to handle both parametric and non-parametric uncertainties, thereby offering greater robustness than traditional control methods. In fact, the synergetic controller demonstrates superior performance in terms of response time and load torque rejection. To further enhance robustness and reduce costs within the vector control framework, the next chapter will focus on the development of a sensorless vector control system for induction motors, employing an fractional adaptive sliding mode observer.

Bibliography

[14] A. A. Kolesnikov, "Introduction of synergetic control," in *2014 American Control Conference*, pp. 3013–3016, IEEE, 2014.

[15] I. Kondratiev and R. Dougal, "General synergetic control strategies for arbitrary number of paralleled buck converters feeding constant power load: Implementation of dynamic current sharing," 2006.

[16] M. Laribi, M. S. Aït Cheikh, C. Larbès, and L. Barazane, "Application de la commande synergétique au contrôle de vitesse d'une machine asynchrone," *Revue des Énergies Renouvelables*, vol. 13, no. 3, pp. 485–493, 2010.

[17] D. Derkouche and K. Kouzi, "Optimized synergetic control approach for a six-phase asynchronous generator coupled to an intelligent flywheel energy storage system," *Revista Română de Informatică şi Automatică*, vol. 32, pp. 103–116, 2022.

[18] M. Boumegouas and K. Kouzi, "A new synergetic scheme control of electric vehicle propelled by six-phase permanent magnet synchronous motor," *Journal Name*, vol. XX, no. YY, pp. ZZ–ZZ, 2020.

[19] A. Yahi and L. Barazane, "Improving speed performances of induction motor by using synergetic control theory," *Journal Name*, vol. XX, no. YY, pp. ZZ–ZZ, 2020.

Chapter 3

Design of an Improved Adaptive Fractional-Order Sliding Mode Observer for Sensorless Control of Induction Motors

3.1 Introduction

Adaptive Sliding Mode Observers (ASMOs) have proven effective in estimating the rotor speed and flux of induction motors (IMs), offering robustness against parameter variations and external disturbances [27] [28]. However, conventional ASMOs rely on integer-order calculus, which may limit their adaptability and dynamic performance in complex scenarios.

To address these limitations, the concept of Fractional Order Control has emerged as a powerful alternative. It is an advanced branch of control theory based on the concept of fractional calculus, which allows differentiation and integration of non-integer order. Unlike traditional control strategies that use only integer-order derivatives and integrals as in classical PID controllers, fractional order control provides additional flexibility by allowing the order of differentiation or integration to be any real (or even complex) number.

The idea of fractional calculus dates back to the 17^{th} century. In 1695, the mathematician Gottfried Wilhelm Leibniz, one of the inventors of calculus, posed a famous question: "What if the order of a derivative is a fraction?"

This marked the origin of fractional calculus. Over the centuries, several mathematicians including Joseph Liouville, Bernhard Riemann, and Paul Lévy contributed to its theoretical development. However, it wasn't until the late 20^{th} century that fractional calculus began to be applied to engineering, thanks to researchers like Igor Podlubny, who formalized the

fractional PID controller $PI^{\lambda}D^{\mu}$, a generalization of the classical PID [20] [21].

Fractional Order Control offers several advantages over classical integer-order methods, including improved flexibility in tuning, better robustness to system uncertainties, and enhanced performance in systems with memory or hereditary properties. However, these benefits come at the cost of increased mathematical complexity and implementation difficulty, especially in real-time applications, due to the need for approximating fractional derivatives and ensuring stability [26] [23].

3.2 Full-State Sliding Mode Adaptive Observer for Induction Machine

The Sliding Mode Observer is illustrated in Figure 3.4. It consists of two blocks: The first relates to the machine model used for estimating the states (rotor flux and stator current), The second handles the adaptation mechanism for estimating the rotor speed [24] [21].

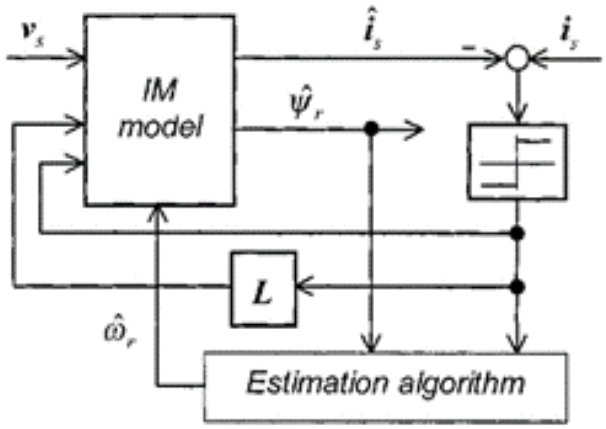

Figure 3.1: Bloc diagram of an adaptive sliding-mode full-state observer for induction motor.

3.3 Full-State Sliding Mode Adaptive Observer for Induction Machine

The dynamics of the induction motor (IM) in the dq reference frame are modeled by:

$$\frac{dx}{dt} = Ax + BU \tag{3.1}$$

The observer estimates the state as [23]:

$$\frac{d\hat{x}}{dt} = \hat{A}\hat{x} + BU + K\,\mathrm{sign}(\hat{i}_s - i_s) \tag{3.2}$$

Where K is a gain matrix defined as:

$$K = \begin{bmatrix} K_1 \\ -LK_1 \end{bmatrix}, \quad \text{with} \quad K_1 = \begin{bmatrix} k_1 & 0 \\ 0 & k_2 \end{bmatrix}, \quad L = \begin{bmatrix} l_{11} & l_{12} \\ l_{21} & l_{22} \end{bmatrix}$$

Then, the error dynamics model is:

$$\frac{de}{dt} = Ae + \Delta A\hat{x} + K\,\text{sign}(\hat{i}_s - i_s) \tag{3.3}$$

With:

$$e = \hat{x} - x = \begin{bmatrix} e_i \\ e_\phi \end{bmatrix}, \quad e_i = \hat{i}_s - i_s, \quad e_\phi = \hat{\phi}_r - \phi_r, \quad \Delta A = \hat{A} - A$$

Assuming the sliding mode condition is fulfilled with a suitably chosen gain matrix K, we can express:

$$e_i = 0, \quad \frac{de_i}{dt} = 0 \tag{3.4}$$

Then, Equation (3.2) yields:

$$0 = A_{12}e_\phi + \Delta A_{11}\hat{i}_s + \Delta A_{12}\hat{\phi}_r - z \tag{3.5}$$

$$\frac{de_\phi}{dt} = A_{22}e_\phi + \Delta A_{21}\hat{i}_s + \Delta A_{22}\hat{\phi}_r + Lz \tag{3.6}$$

Where:

$$z = -k\,\text{sign}(\hat{i}_s - i_s)$$

Assuming the rotor speed is known and all IM parameters are constant, the rotor flux dynamic error under sliding conditions becomes:

$$\frac{de_\phi}{dt} = (A_{22} + LA_{12})e_\phi \tag{3.7}$$

Now, suppose the rotor speed is variable. The variation in the system matrix is:

$$\Delta A = \begin{bmatrix} 0 & -\frac{\Delta\omega_r}{\varepsilon}J \\ 0 & \Delta\omega_r J \end{bmatrix}, \quad J = \begin{bmatrix} 0 & -1 \\ 1 & 0 \end{bmatrix}, \quad \Delta\omega_r = \hat{\omega}_r - \omega_r$$

The Lyapunov function is selected as:

$$V = \frac{1}{2}e_\phi^T e_\phi + \frac{1}{2\varepsilon\mu}(\Delta\omega_r)^2 \tag{3.8}$$

Let us compute the derivative of V [26][20]:

$$\frac{dV}{dt} = \left(\frac{de_\phi}{dt}\right)^T e_\phi + \frac{1}{\varepsilon\mu}\frac{d(\Delta\omega_r)}{dt}\Delta\omega_r \tag{3.9}$$

This can be written as:

$$\frac{dV}{dt} = \frac{dV_1}{dt} + \frac{dV_2}{dt}$$

With:

$$\frac{dV_1}{dt} = z^T \Lambda^T A_{12}^{-1} z, \quad \frac{dV_2}{dt} = z^T \Lambda^T A_{12}^{-1} \frac{\Delta\omega_r}{\varepsilon} J\hat{\phi}_r + \frac{1}{\varepsilon\mu} \frac{d(\Delta\omega_r)}{dt} \Delta\omega_r$$

Where $\Lambda = L - \varepsilon I$. The observer stability is guaranteed if $\frac{dV}{dt} < 0$. One solution is to select:

$$\frac{dV_1}{dt} < 0 \quad \text{and} \quad \frac{dV_2}{dt} = 0$$

A sufficient condition is to define:

$$\Lambda^T = -\gamma A_{12}$$

Where γ is a positive design parameter [30] [21] [24].

Under these conditions, the rotor speed estimation is expressed as:

$$\frac{d\hat{\omega}_r}{dt} = \mu\gamma \left(k_1 \operatorname{sign}(\hat{i}_{s\alpha} - i_{s\alpha})\, \hat{\phi}_{r\beta} - k_2 \operatorname{sign}(\hat{i}_{s\beta} - i_{s\beta})\, \hat{\phi}_{r\alpha} \right) \tag{3.1}$$

$$\hat{\omega}_r = \int \mu\gamma \left(k_1 \operatorname{sign}(\hat{i}_{s\alpha} - i_{s\alpha})\, \hat{\phi}_{r\beta} - k_2 \operatorname{sign}(\hat{i}_{s\beta} - i_{s\beta})\, \hat{\phi}_{r\alpha} \right) dt \tag{3.10}$$

3.4 Fractional Order Calculus

The Grünwald–Letnikov fractional derivative of order μ of a function $f(t)$ is defined as [20]:

$$D_t^\mu f(t) = \lim_{h \to 0} \frac{1}{h^\mu} \sum_{k=0}^{\lfloor t/h \rfloor} (-1)^k \binom{\mu}{k} f(t - kh) \tag{3.11}$$

Where:

- $\mu \in \mathbb{R}$ is the fractional order,
- $\binom{\mu}{k}$ is the generalized binomial coefficient defined by:

$$\binom{\mu}{k} = \frac{\Gamma(\mu + 1)}{\Gamma(k + 1)\Gamma(\mu - k + 1)} \tag{3.12}$$

Where $\Gamma(\cdot)$ is the gamma function, given by:

$$\Gamma(x) = \int_0^\infty t^{x-1} e^{-t} dt \tag{3.13}$$

3.5 Fractional Adaptive Sliding Mode Observer for Induction Motor

The FOASMO proposed here is a modification of the conventional sliding-mode observer [23] [30], where the discontinuous switching term $\text{sign}(i_s - \hat{i}_s)$ is replaced by a smooth exponential integral of the error. This change aims to reduce the high-frequency chattering typically caused by the abrupt nature of the sign function.

In this approach, the error between the measured and estimated stator current components, $e_1 = i_{s\alpha} - \hat{i}_{s\alpha}$ and $e_2 = i_{s\beta} - \hat{i}_{s\beta}$, is used as input to a continuous correction law defined by an exponentially weighted integral. This formulation ensures a gradual response instead of a discontinuous switching action.

The correction term is applied to the observer as follows:

$$u_i(t) = -K_i \left(\int e(t)\, dt \right)^{\lambda}, \quad i = 1, 2 \tag{3.14}$$

Where K_i are observer gains, and $\lambda > 0$ is the exponential decay rate controlling the memory of past errors. The output of this integral replaces the sign function in the sliding surface of the observer and improves system smoothness and robustness.

To further enhance the estimation dynamics, the observer uses fractional-order derivatives in its structure. This inclusion allows the observer to benefit from the memory and adaptability characteristics of fractional calculus, particularly useful under variable speed and parameter deviation conditions.

3.6 Simulation Results and Discussion

To evaluate the performance and robustness of the proposed FOASMO, a series of simulation tests were conducted under various dynamic operating conditions. These tests aim to verify the effectiveness of the fractional-order approach and to demonstrate the closed-loop stability of the system. The scenarios include sudden changes in speed commands, step changes in load torque, and variations in motor parameters.

In this section, we present and compare the estimated speed versus actual speed results for both the classical Adaptive Sliding Mode Observer (ASMO) and the proposed Fractional-Order Adaptive Sliding Mode Observer (FOASMO). The estimation results obtained using the FOASMO are shown in Figure 3.3, while those corresponding to the ASMO are illustrated in Figure 3.2, enabling a direct comparison of their performance.

In the first step, a direct comparison between the FOASMO and the classical SMO was performed. It is observed that the FOASMO provides a faster and smoother transient re-

sponse with significantly reduced chattering in the estimated speed signal. This confirms the benefit of replacing the sign function with an exponentially weighted integral.

These results clearly illustrate that the proposed FOASMO outperforms the conventional SMO in terms of estimation precision, chattering elimination, and resilience to parameter uncertainties.

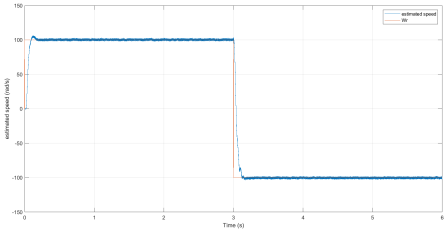

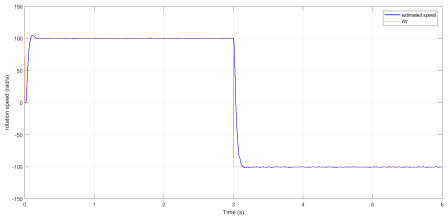

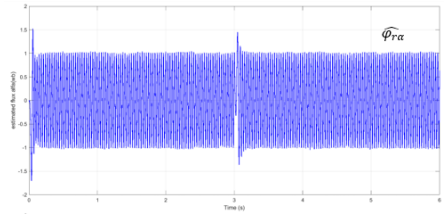

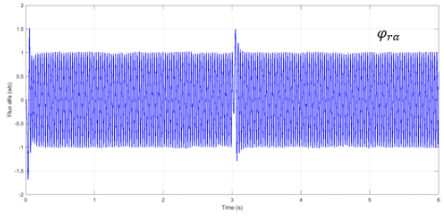

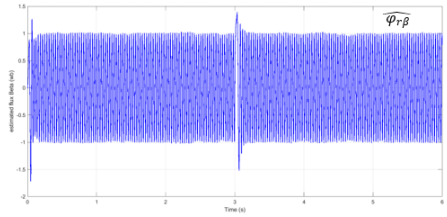

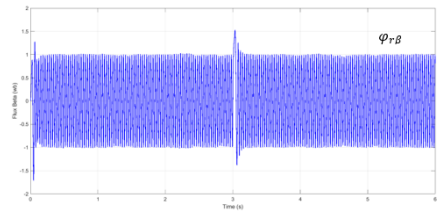

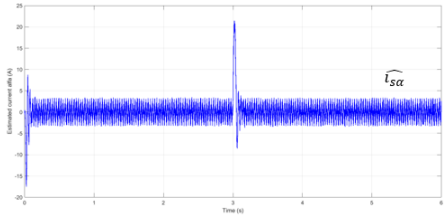

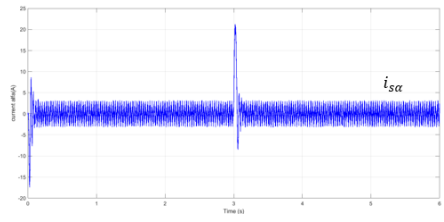

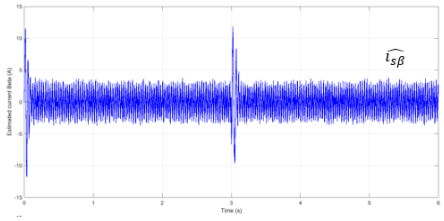

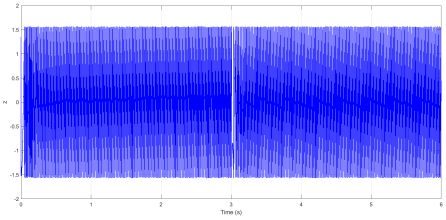

Simulation Results of ASMO Estimator Performance

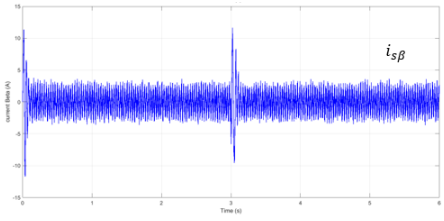

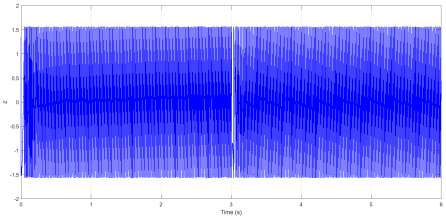

Simulation Results of ASMO

Figure 3.2: Simulation Results: ASMO Estimated vs Actual

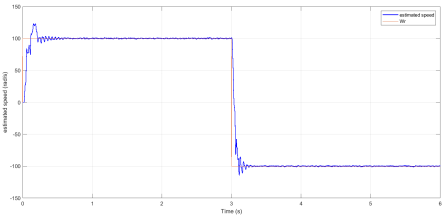

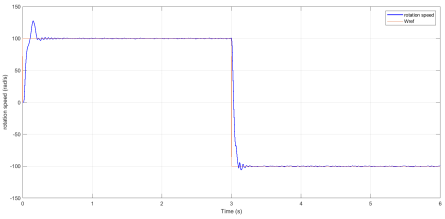

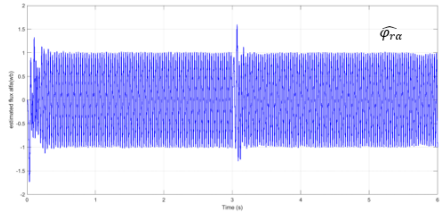

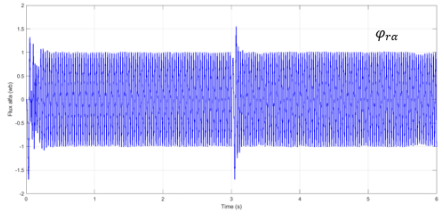

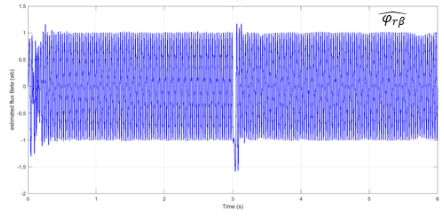

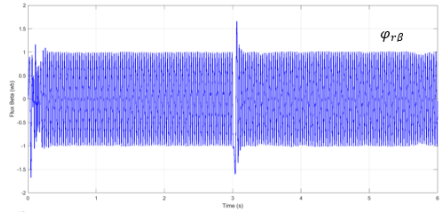

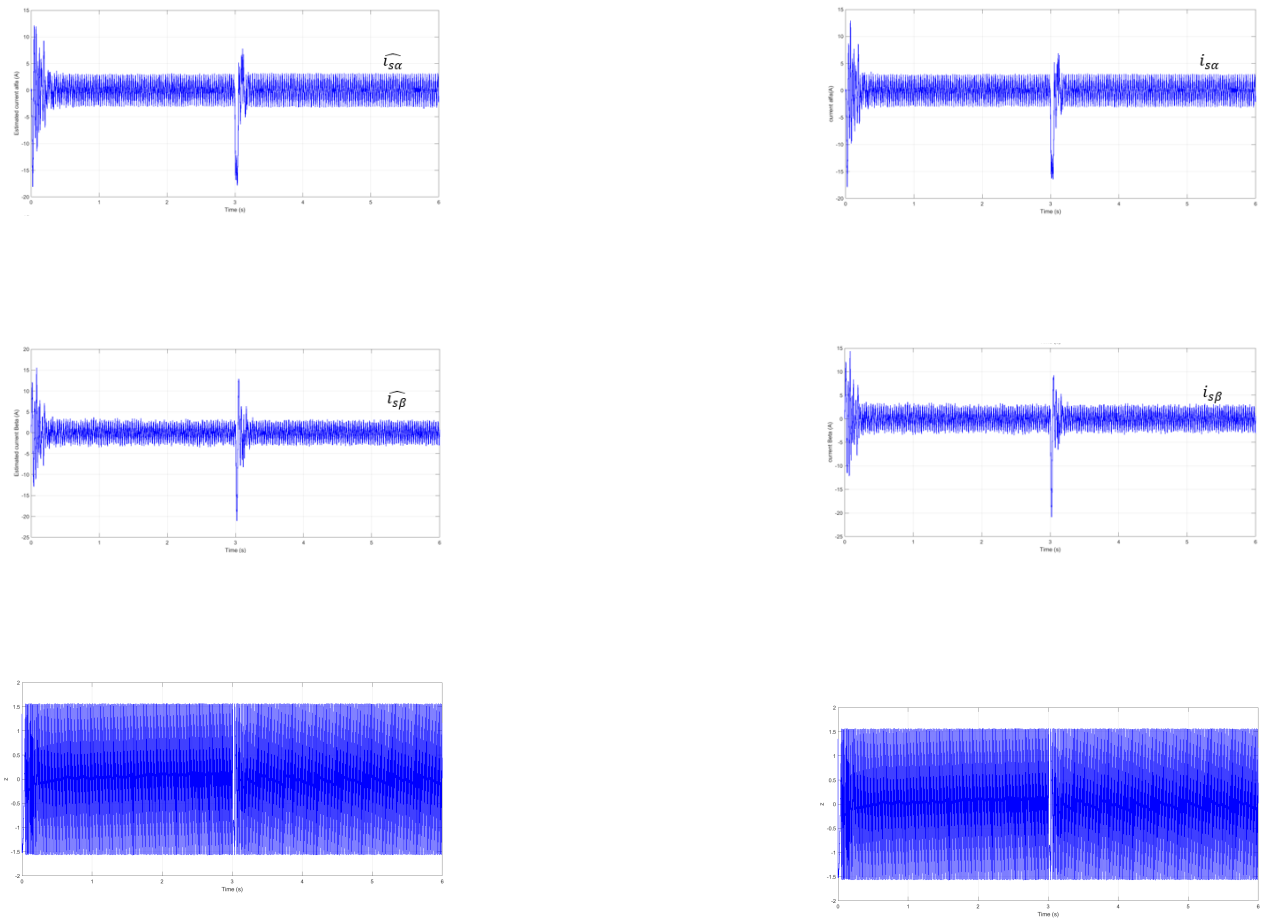

Simulation Results of FOASMO Estimator Performance

Simulation Results of FOASMO

Figure 3.3: Simulation Results: FOASMO Estimated vs Actual

3.6.1 Speed Maximum Dynamic Error

To evaluate the performance of the proposed estimation algorithm in terms of the **maximum dynamic speed error**, the algorithm was tested and compared under load conditions with that of the reference [23], for different values of the **reference speed** and the **observer design constant** $\mu.\lambda$, as shown in Figure 3.3.

According to the figure, it is observed that **speed estimation is significantly improved at low speeds** thanks to the use of the FO-ASMO algorithm. In fact, with the FO-ASMO, the **maximum dynamic error remains very low and almost constant** throughout the entire speed range. At very low speed (5 rad/s), the error is about **0.0045%**, compared to **0.041%** for the classical ASMO. At the nominal speed (100 rad/s), the error does not exceed **0.004%** in both cases, but remains slightly lower when using the fractional-order observer.

Unlike the classical ASMO, which exhibits relatively high error at low speeds and more noticeable variations, the **FO-ASMO algorithm demonstrates better robustness and dynamic stability**.

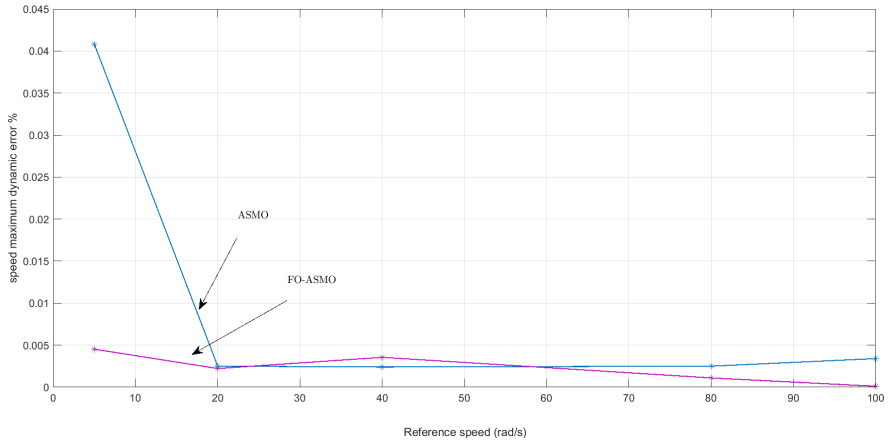

Figure 3.4: Speed maximum dynamic error at load operation Versus reference speed.

3.7 Conclusion

This chapter presented the Adaptive Sliding Mode Observer (ASMO) and discussed its chattering issue, which can degrade estimation quality. To address this, a Fractional-Order Adaptive Sliding Mode Observer (FO-ASMO) was introduced, significantly reducing chattering while preserving accurate and robust speed and flux estimation. The results confirm that this improved observer enables smooth, sensorless control of the induction machine across its entire operating range.

Bibliography

[20] I. Podlubny, *Fractional-Order Systems and Fractional-Order Controllers*, Slovak Academy of Sciences, Institute of Experimental Physics, Košice, Slovakia, 1994.

[21] K. Kouzi, *Contribution des techniques de la logique floue pour la commande d'une machine à induction sans transducteur rotatif*, Master's thesis, University of Elhadj Lakhdar, Batna, Algeria.

[22] M. K. B. Boumegouas, *Contribution of advanced control techniques to the diagnosis, estimation, and management of an electric vehicle chain*, Ph.D. dissertation, Dept. of Electrical Engineering, Amar Telidji Univ., Laghouat, Algeria, 2025.

[23] M. Tursini, R. Petrella, and F. Parasiliti, "Adaptive sliding mode observer for speed sensorless control of induction motors," *IEEE Trans. Ind. Appl.*, vol. 36, no. 5, pp. 1380–1387, Sep./Oct. 2000.

[24] A. Aoufi, *Utilisation d'observateurs à modes glissants pour le contrôle direct de couple et le contrôle vectoriel d'une machine asynchrone à cage*, Master's thesis, [Institution missing].

[25] K. Kouzi, L. Mokrani, and M.-S. Naït-Saïd, "A rotor flux sliding-mode observer for a fuzzy logic control of direct field oriented induction motor," In *International Conference on Electrical and Electronics Engineering*, Sétif, October 2004.

[26] K. Kouzi, L. Mokrani, and M.-S. Naït-Saïd, "Adaptive sliding-mode observer for speed sensorless control of induction motors," *IEEE Transactions on Industry Applications*, vol. 36, no. 5, pp. 1380–1387, 2000.

[27] C. Vasilios, "PMSM sensorless control on sliding mode observers methodology for non-linear system with model imprecision," In *International Workshop on Recent Advances in Sliding Modes (RASM)*, 2015.

[28] K. Hongryel, S. Jubum, and L. Jangmyung, "High speed sliding mode observer for the sensorless speed control of a PMSM," *IEEE Transactions on Industrial Electronics*, vol. 58, no. 9, pp. 4096–4107, 2011.

[29] K. Kouzi and M.-S. Naït-Saïd, "Adaptive Fuzzy Logic Speed-Sensorless Control Improvement of Induction Motor Drives for Standstill and Low Speed Operations," *International Journal COMPEL*, vol. 26, no. 1, pp. 22–33, Jan. 2007.

[30] K. Kouzi, M.-S. Naït-Saïd, M. Hilairet, and A. Berthelot, "A Fuzzy Sliding Mode Adaptive Speed Observer for Vector Control of an Induction Motor," 2008.

GENERAL CONCLUSION

The study presented in this work focuses on the implementation of a robust synergetic sensorless vector control strategy for the induction motor, based on an integral fractional-order adaptive sliding mode observer. The performance of the proposed sensorless scheme, particularly in terms of speed estimation accuracy, has been thoroughly evaluated, especially under low-speed operation and during reference speed variations.

In high-performance applications, induction motors are commonly controlled using the vector control technique. The fundamental principle of this method is to decompose the stator current vector into two orthogonal components: one responsible for controlling the magnetic flux, and the other for regulating the electromagnetic torque. This decoupling enables independent control of torque and flux, resulting in dynamic performance similar to that of a separately excited DC motor.

However, vector control requires accurate measurement or estimation of rotor speed and flux to achieve high-performance induction motor (IM) drives. Direct measurement poses several challenges, including the high cost and fragility of sensors. Additionally, harsh operating environments and space constraints often limit the feasibility of sensor installation. As a result, sensorless control emerges as an attractive solution, offering reduced implementation costs and allowing practitioners to overcome practical limitations such as limited space and exposure to severe environmental conditions.

To achieve this objective, the first chapter of this work was devoted to the modeling of the induction motor (IM) using Park's model, followed by the application of a decoupled control strategy. The chapter concluded with simulation results that illustrate the key performance benefits of vector control.

The second chapter was dedicated to presenting the theory of synergetic control applied to IM drives. The control strategy offers high performance in terms of tracking accuracy and robustness. The effectiveness of this approach was validated through numerical simulation results.

To reduce the overall control cost by eliminating the speed sensor, and to enhance estimation accuracy particularly at low speeds, an integral fractional-order adaptive sliding

mode observer was developed for IM speed estimation. The proposed observer estimates the rotor flux components in the stationary reference frame, while the rotor speed is estimated using a Lyapunov-based approach. The performance and robustness of the observer were demonstrated through simulation results under various operating conditions.

Perspectives

Regarding the continuation of this work, several perspectives can be explored:

- Development of algebraic observer for of IM;
- Design of fault tolerant control: Enhancing the robustness of the system by integrating fault detection and tolerance mechanisms, particularly for sensor and IM faults;
- Development of an intelligent vector control of IM using internet of things;
- Experimental Validation: Implementing the proposed control and observer schemes on a real-time test bench to validate their performance under practical conditions.

Annexes

Induction Motor Parameters

Parameter	**Value**
Number of pole pairs	2
Nominal speed (tr/min)	1400
Rated power (kW at 50 Hz)	0.75
Nominal voltage (V)	220 / 380
Nominal current (A)	3.6 / 2.1
Nominal torque (Nm)	5
Stator resistance R_s (Ω)	10
Rotor resistance R_r (Ω)	6.3
Stator inductance L_s (H)	0.656
Rotor inductance L_r (H)	0.653
Mutual inductance M (H)	0.612
Moment of inertia J ($\mathrm{kg} \cdot \mathrm{m}^2$)	0.02
Friction coefficient f_s ($\mathrm{N} \cdot \mathrm{m} \cdot \mathrm{s}$)	0

Parameters of the tested induction motor.

System Parameters

- **Three-Phase Network Parameters:** 220/380 V ; 50 Hz
- **Inverter Parameters:** $\Delta i = 0.1$ A (Hysteresis Band)
- **Filter Parameters:**
  - Capacitance: $C = 6 \times 10^{-3}$ F
  - Inductance: $L = 1.2 \times 10^{-3}$ H